

LA-UR- 04-0525

Approved for public release;
distribution is unlimited.

Title: Creation of a Simplified Benchmark Model for the Neptunium
Sphere Experiment

Author(s): Russell D. Mosteller
David J. Loaiza
Rene G. Sanchez

Submitted to: PHYSOR 2004: The Physics of Fuel Cycles and Advanced
Nuclear Systems: Global Developments
Chicago, IL
April 25 - 29, 2004

LOS ALAMOS NATIONAL LABORATORY



3 9338 00454 2436



Los Alamos National Laboratory, an affirmative action/equal opportunity employer, is operated by the University of California for the U.S. Department of Energy under contract W-7405-ENG-36. By acceptance of this article, the publisher recognizes that the U.S. Government retains a nonexclusive, royalty-free license to publish or reproduce the published form of this contribution, or to allow others to do so, for U.S. Government purposes. Los Alamos National Laboratory requests that the publisher identify this article as work performed under the auspices of the U.S. Department of Energy. Los Alamos National Laboratory strongly supports academic freedom and a researcher's right to publish; as an institution, however, the Laboratory does not endorse the viewpoint of a publication or guarantee its technical correctness.

Form 836 (8/00)

Creation of a Simplified Benchmark Model for the Neptunium Sphere Experiment

Russell D. Mosteller, David J. Loaiza, and Rene G. Sanchez
Los Alamos National Laboratory, P. O. Box 1663, Los Alamos, NM 87545 USA

Although neptunium is produced in significant amounts by nuclear power reactors, its critical mass is not well known. In addition, sizeable uncertainties exist for its cross sections. As an important step toward resolution of these issues, a critical experiment was conducted in 2002 at the Los Alamos Critical Experiments Facility. In the experiment, a 6-kg sphere of ^{237}Np was surrounded by nested hemispherical shells of highly enriched uranium. The shells were required in order to reach a critical condition.

Subsequently, a detailed model of the experiment was developed. This model faithfully reproduces the components of the experiment, but it is geometrically complex. Furthermore, the isotopics analysis upon which that model is based omits nearly 1% of the mass of the sphere.

A simplified benchmark model has been constructed that retains all of the neutronic aspects of the detailed model and substantially reduces the computer resources required for the calculation. The reactivity impact of each of the simplifications is quantified, including the effect of the missing mass. A complete set of specifications for the benchmark is included in the full paper.

Both the detailed and simplified benchmark models underpredict k_{eff} by more than 1% Δk . This discrepancy supports the suspicion that better cross sections are needed for ^{237}Np .

Creation of a Simplified Benchmark Model for the Neptunium Sphere Experiment

Russell D. Mosteller^{*1}, David J. Loaiza,¹ and Rene G. Sanchez¹

¹*Los Alamos National Laboratory, P. O. Box 1663, Los Alamos, NM 87545 USA*

A simplified benchmark model has been constructed for a critical experiment in which a 6-kg sphere of ^{237}Np was surrounded by nested hemishells of highly enriched uranium. The simplified benchmark model retains all of the neutronic important aspects of the detailed model of the experiment and substantially reduces the computer resources required for the calculation. However, both the detailed and simplified benchmark models underpredict k_{eff} by more than 1% Δk . This discrepancy supports the suspicion that better cross sections are needed for ^{237}Np .

KEYWORDS: *Neptunium, Criticality, Benchmarks, MCNP*

1. Introduction

Although neptunium is produced in significant amounts by nuclear power reactors, its critical mass is not well known. In addition, sizeable uncertainties exist for its cross sections. As an important step toward resolution of these issues, a critical experiment was conducted in 2002 at the Los Alamos Critical Experiments Facility (LACEF). In the experiment, a 6-kg sphere of ^{237}Np was surrounded by nested hemispherical shells of highly enriched uranium (HEU). [1-4] The HEU shells were required in order to reach a critical condition.

Subsequently, a detailed model of the experiment was developed [5]. This model faithfully reproduces the components of the experiment, but it is geometrically complex. Furthermore, the isotopics analysis upon which that model is based omits nearly 1% of the mass of the sphere. The objective of the study reported herein was to produce a simplified benchmark model that removes the geometric complexity but retains all the important aspects of its neutronic behavior. As part of that process, the reactivity impact of the missing mass has been quantified.

2. Description of Experiment

The experiment was performed on the Planet vertical assembly at LACEF. The Planet assembly has two primary components: a stationary platform that supports a stainless-steel membrane to hold the upper portion of the experimental assembly in place, and a vertical drive that lifts the lower portion of the assembly upward. In this particular experiment, the upper portion of the assembly contained 14 hemispherical HEU shells, while the lower portion contained 15 hemispherical HEU shells and the neptunium sphere. An aluminum spacer was placed on top of the lower HEU shells to prevent a configuration that would exceed operating limits. The neptunium sphere was enclosed in a tungsten shell to reduce the radiological hazard, and that shell, in turn, was coated with two

^{*} Corresponding author, Tel. 505-665-4879, FAX 505-665-3046, E-mail: mosteller@lanl.gov

separate layers of nickel cladding. A slightly idealized schematic of the experimental configuration is shown in Figure 1.

3. Benchmark Simplifications

Three sequential steps were taken to produce a simplified benchmark model. First, the impact of the missing mass was assessed. Next, a set of geometric approximations was introduced, and the reactivity impact of those approximations was quantified. Finally, a series of material simplifications was incorporated, and the reactivity impact of those approximations was determined.

All of the calculations were performed with the MCNP5™ Monte Carlo code [6] and a combination of the ACTI [7] and ENDF66 [8] nuclear data libraries that corresponds to the final version of ENDF/B-VI [9]. Each calculation employed 650 generations of 10,000 neutrons each, and the results from the first 50 generations were discarded. Consequently, the results from each case are based on 6,000,000 active neutron histories.

Previous simplifications were retained at each step in the process. Consequently, the standard deviations associated with the calculations are not compounded, and the results from any step can be compared directly with those from any other step.

3.1 Missing Mass

The composition of the sphere was determined from a chemical assay of the sprue. Unfortunately, that sample did not dissolve completely, leaving 0.946 wt.% of the mass of the sphere unaccounted for. The “missing” mass could be any of a number of components or some combination of them. The sphere was cast in a graphite mold with a lining of erbia power. In

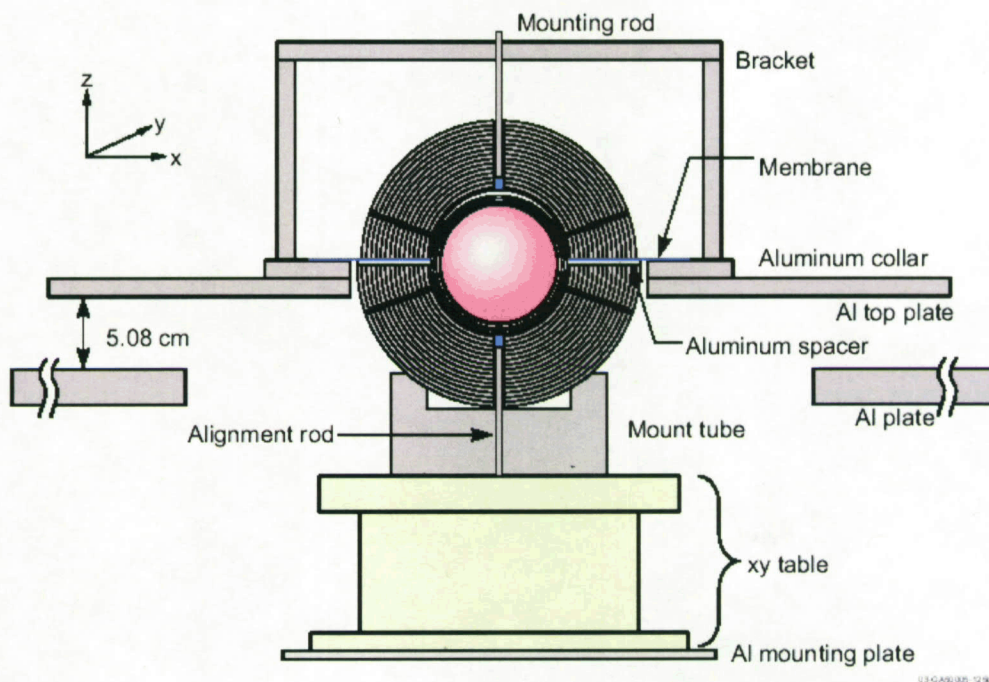


Fig. 1 Schematic of the Experiment.

addition, iron is a common impurity from the casting process, and it has been reported that europium is often a contaminant in neptunium refined from spent reactor fuel [10]. Alternatively, it is possible that the undissolved material was very similar to the dissolved portion and was effectively pure neptunium.

MCNP5 calculations were performed to assess the reactivity impact of these alternatives, and the results from those calculations are presented in Table 1. It is clear that the impact of the missing mass is quite small, irrespective of its actual composition. Based on the results from that table, representing the missing mass as void, with an associated uncertainty of $\pm 0.0012 \Delta k$, appears to be an adequate approximation. The benchmark value of k_{eff} for the detailed model of the experiment previously was determined to be 1.0026 ± 0.0034 [4], based on the measured excess reactivity and the uncertainties associated with the experiment. When the additional uncertainty for the missing mass is folded into that value, the final benchmark value of k_{eff} for the detailed model becomes 1.0026 ± 0.0036 .

3.2 Geometric Simplifications

The geometric simplifications that were made and their corresponding impact on reactivity are summarized in Table 2. Some structural components and the aluminum spacer were retained because their removal produces a reactivity change that is unacceptably large. Removal of the spacer, for example, increases reactivity by approximately 1% Δk . Similarly, complete removal of the bridge base, collar, and platform produces an unacceptable reduction in reactivity. Instead, they have been combined into a single ring that approximately conserves the cumulative reactivity contribution from all three.

The simplifications that produce the largest reactivity changes are the removal of the X-Y alignment table, the aluminum stems, and the steel membrane. However, none of the reactivity changes for any individual simplification exceeds $\pm 0.0020 \Delta k$, and the net effect of all of them is only $-0.0015 \pm 0.0003 \Delta k$.

3.3 Material Simplifications

The detailed model of the experiment [5] explicitly represents each HEU hemishell with its own dimensions and mass. It also explicitly represents the gaps between the hemishells, as well as the gaps between the neptunium sphere and each layer of its cladding.

Table 1 Reactivity Effect of Missing Mass.

| Missing mass represented as | Δk | Fission Fraction | |
|-----------------------------|----------------------|-------------------|------------------|
| | | ^{237}Np | ^{235}U |
| Void | — | 0.1264 | 0.857 |
| Carbon | -0.0005 ± 0.0004 | 0.1257 | 0.8577 |
| Iron | -0.0002 ± 0.0004 | 0.1257 | 0.8576 |
| Europium | -0.0011 ± 0.0004 | 0.1258 | 0.8576 |
| Erbium* | 0.0004 ± 0.0004 | 0.1259 | 0.8574 |
| ^{237}Np | 0.0012 ± 0.0004 | 0.1278 | 0.8556 |

* Only ^{166}Er and ^{167}Er present

Table 2 Reactivity Impact of Geometric Simplifications.

| Change | Δk |
|--|----------------------|
| Remove bridge | -0.0001 ± 0.0003 |
| Remove mounting plate | -0.0007 ± 0.0003 |
| Remove aluminum support plate | -0.0002 ± 0.0003 |
| Remove X-Y alignment table | -0.0018 ± 0.0003 |
| Remove empty holes in HEU hemishells | 0.0002 ± 0.0003 |
| Remove aluminum stems | -0.0010 ± 0.0003 |
| Simplify aluminum mounting tube | 0.0001 ± 0.0003 |
| Remove membrane | 0.0014 ± 0.0003 |
| Convert bridge base, collar, and top plate into cylindrical ring | 0.0006 ± 0.0003 |
| Cumulative change | -0.0015 ± 0.0003 |

The density of the HEU hemishells first was changed to a uniform average value, although their thicknesses still varied from one hemishell to another. Subsequently, the hemishells were homogenized with the gaps between them to produce a single homogeneous hemisphere for the lower hemishells and another such hemisphere for the upper hemishells. Next, the aluminum liners were homogenized with the gaps around them to create homogeneous regions that fit snugly against the homogenized HEU hemispheres. The homogenization of the lower aluminum liner also included the gap between it and the nickel cladding of the sphere. However, the gap between the aluminum liner for the upper HEU hemishells and the nickel cladding was retained in the benchmark model. It is relatively large and irregularly shaped, and homogenizing it with that aluminum liner would have distorted the distribution of the aluminum without reducing the geometric complexity of the model in any meaningful way. Finally, the tungsten cladding was homogenized with the gap between it and the neptunium sphere, and the two layers of nickel were homogenized with the gaps they enclose.

The reactivity changes from these simplifications are summarized in Table 3. Homogenizing the HEU hemishells with the gaps they enclose increases reactivity slightly, which is not surprising because, on average, it moves the uranium slightly inward toward the neptunium sphere. The impact of the other changes is much smaller, but in the aggregate they partially offset the effect of homogenizing the HEU hemishells. The net effect is a reactivity change of only $0.0008 \pm 0.0004 \Delta k$.

3.4 Cumulative Effect of Simplifications

The results from Tables 2 and 3 can be combined to produce the final bias for the simplified benchmark model, as shown in Table 4. From section 3.1, the benchmark value of k_{eff} for the detailed model is 1.0026 ± 0.0036 . Based on the cumulative reactivity impact of the simplifications, the benchmark value of k_{eff} for the simplified benchmark model therefore is 1.0019 ± 0.0036 .

Table 3 Reactivity Impact of Material Simplifications.

| Change | Δk |
|--|----------------------|
| Average density for all HEU hemishells | -0.0001 ± 0.0003 |
| Homogenize HEU hemishells with enclosed gaps | 0.0016 ± 0.0003 |
| Homogenize aluminum liners with gaps | -0.0002 ± 0.0003 |
| Homogenize tungsten and nickel cladding with enclosed gaps | -0.0005 ± 0.0004 |
| Cumulative change | 0.0008 ± 0.0004 |

Table 4 Cumulative Reactivity Impact of Simplifications.

| Change | Δk |
|---------------------------|----------------------|
| Geometric simplifications | -0.0015 ± 0.0003 |
| Material Simplifications | 0.0008 ± 0.0004 |
| Cumulative change | -0.0007 ± 0.0004 |

4. Calculated Results for the Detailed and Simplified Benchmark Models

After the simplified benchmark model had been determined, the MCNP input file was revised to make it as simple as possible while retaining complete consistency with the specifications for the simplified benchmark model. The results from that model are compared with those from the detailed model in Table 5. The comparison clearly demonstrates the equivalence of the two representations. Furthermore, the simplified benchmark consumes less than 40% as much CPU time as the detailed model. A schematic of the simplified benchmark model is shown in Figure 2, and a detailed set of specifications is provided in the Appendix.

As Table 5 indicates, the calculated values for k_{eff} for the detailed and benchmark models are 0.9896 ± 0.0002 and 0.9889 ± 0.0002 , respectively. Consequently, the magnitude of the difference between the calculated and benchmark values for k_{eff} is more than 1% Δk , and it also is more than four times the standard deviation associated with the benchmark value. That discrepancy supports the suspicion that better cross sections are needed for ^{237}Np .

5. Summary and Conclusions

A simplified benchmark model has been constructed for the Np sphere experiment. The model allows for the 0.946 wt.% of the mass of the sphere that is unaccounted for, and it has simplified representations for both the geometry of the experiment and the materials that comprise it. Furthermore, it retains all of the important neutronic aspects of the experiment, and it substantially reduces the computer resources required for the calculation.

The calculated results for both the detailed and simplified benchmark models underpredict k_{eff} by more than 1% Δk . This discrepancy supports the suspicion that better cross sections are needed for ^{237}Np .

Table 5 Comparison of Results from Detailed and Simplified Benchmark Models.

| Parameter | | Model | |
|--|------------------|---------------------|----------------------|
| | | Detailed | Simplified Benchmark |
| k_{eff} | | 0.9896 ± 0.0002 | 0.9889 ± 0.0002 |
| Fission Distribution, by Energy | Fast | 0.9476 | 0.9478 |
| | Intermediate | 0.0524 | 0.0522 |
| | Thermal | 0.0 | 0.0 |
| Fission Fraction, by Material | Np | 0.1251 | 0.1255 |
| | ^{235}U | 0.8584 | 0.8580 |
| Average Energy of Neutrons Causing Fission (MeV) | | 1.516 | 1.519 |
| Average Number of Neutrons Produced per Fission | | 2.636 | 2.637 |
| Execution Time (CPU Minutes)* | | 74.25 | 27.50 |

*Calculations were performed on an 800 MHz PC running Windows 2000 Professional

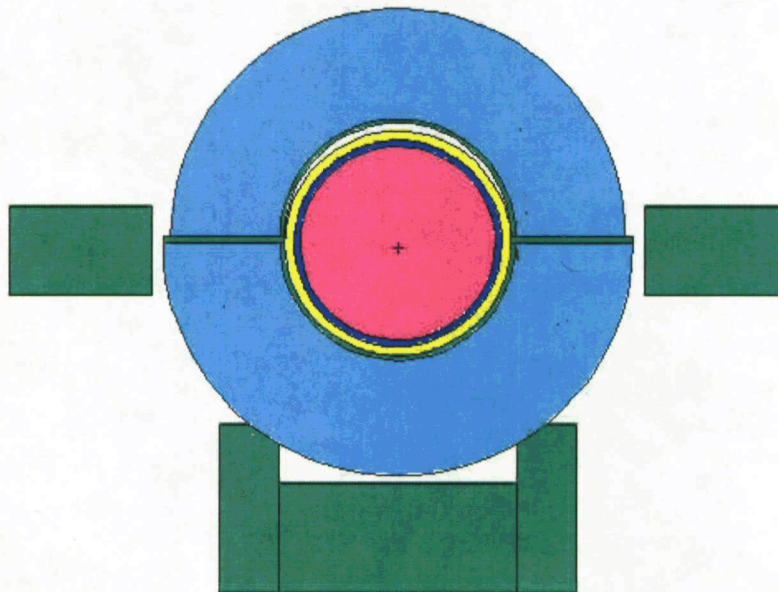


Fig. 2 Two-Dimensional Schematic of the Simplified Benchmark Model.

A.1 Dimensions

Dimensions for the spheres and hemispheres are given in Table A-1, and those for the cylinders are given in Table A-2. The position of the cylindrical aluminum ring is such that its top is 1.5875 cm above the center of the neptunium sphere, and its bottom is 2.2225 cm below it.

A.2 Densities

The compositions of each of the materials in the final model are given in Tables A-3 through A-7. The chemical composition of the two aluminum liners in Table A-6 is identical, but the lower liner has been homogenized with a larger void region than has the upper. Consequently, the density of the homogenized lower liner is only 0.91753 times that of the upper one.

Table A-1 Radii of Spheres and Hemispheres.

| Region | Inner Radius (cm) | Outer Radius (cm) |
|----------------------|-------------------|-------------------|
| Neptunium Sphere | — | 4.14909 |
| Tungsten Cladding | 4.14909 | 4.42722 |
| Nickel Cladding | 4.42722 | 4.81838 |
| Lower Aluminum Liner | 4.81838 | 5.01700 |
| Lower HEU Hemisphere | 5.01700 | 10.00000 |
| Upper Aluminum Liner | 4.83108 | 5.01300 |
| Upper HEU Hemisphere | 5.01300 | 9.66800 |

Table A-2 Dimensions of Cylinders.

| Region | Inner Radius (cm) | Outer Radius (cm) | Height (cm) |
|---------------------------|-------------------|-------------------|-------------|
| Aluminum Shim | 5.08000 | 10.00000 | 0.31750 |
| Aluminum Ring | 10.47750 | 16.51000 | 3.81000 |
| Upper Portion of Pedestal | 5.08000 | 7.62000 | 2.54000 |
| Lower Portion of Pedestal | — | 7.62000 | 4.76250 |

Table A-3 Composition of the Neptunium Sphere.

| Isotope | Number Density (atoms/b-cm) |
|-------------------|--------------------------------|
| ²³³ U | 1.8577×10^{-6} |
| ²³⁴ U | 2.9633×10^{-7} |
| ²³⁵ U | 1.4074×10^{-5} |
| ²³⁶ U | 7.8349×10^{-8} |
| ²³⁸ U | 1.5626×10^{-6} |
| ²³⁷ Np | 5.0926×10^{-2} |
| ²³⁸ Pu | 8.2304×10^{-7} |
| ²³⁹ Pu | 1.6271×10^{-5} |
| ²⁴⁰ Pu | 1.1619×10^{-6} |
| ²⁴¹ Pu | 3.1166×10^{-8} |
| ²⁴² Pu | 1.6032×10^{-7} |
| ²⁴¹ Am | 3.3375×10^{-7} |
| ²⁴³ Am | 9.1575×10^{-5} |

Table A-4 Composition of the Homogenized Tungsten Cladding.

| Isotope or Element | Number Density (atoms/b-cm) |
|-----------------------|--------------------------------|
| Iron | 3.4491×10^{-3} |
| Nickel | 3.2820×10^{-3} |
| ¹⁸² W | 1.4057×10^{-2} |
| ¹⁸³ W | 7.5931×10^{-3} |
| ¹⁸⁴ W | 1.6254×10^{-2} |
| ¹⁸⁶ W | 1.5079×10^{-2} |

Table A-5 Composition of the Homogenized Nickel Cladding.

| Element | Number Density (atoms/b-cm) |
|---------|--------------------------------|
| Nickel | 8.5344×10^{-2} |

Table A-6 Composition of Al-6061-T6 for the Homogenized Liners.

| Isotope or Element | Number Density (atoms/b-cm) | |
|-----------------------|-----------------------------|-------------------------|
| | Upper Liner | Lower Liner |
| Magnesium | 7.1200×10^{-4} | 6.5328×10^{-4} |
| ^{27}Al | 5.5475×10^{-2} | 5.0900×10^{-2} |
| Silicon | 3.2862×10^{-4} | 3.0152×10^{-4} |
| Titanium | 2.4102×10^{-5} | 2.2114×10^{-5} |
| Chromium | 5.7689×10^{-5} | 5.2931×10^{-5} |
| ^{55}Mn | 2.1000×10^{-5} | 1.9268×10^{-5} |
| Iron | 9.6403×10^{-5} | 8.8452×10^{-5} |
| Copper | 6.6568×10^{-5} | 6.1078×10^{-5} |

Table A-7 Composition of the HEU Hemispheres.

| Isotope | Number Density (atoms/b-cm) |
|------------------|--------------------------------|
| ^{234}U | 4.7468×10^{-4} |
| ^{235}U | 4.3169×10^{-2} |
| ^{236}U | 2.1687×10^{-4} |
| ^{238}U | 2.4478×10^{-3} |